

# All-polarization-maintaining, SESAM mode-locked femtosecond Er-doped fiber laser with gigahertz fundamental repetition rate

Jiazheng Song<sup>1,2</sup>, Xiaohong Hu<sup>1</sup>, Hushan Wang<sup>1</sup>, Ting Zhang<sup>1</sup>, Yishan Wang<sup>1</sup>,  
Yuanshan Liu<sup>3,\*</sup>, Jianguo Zhang<sup>1,4,5</sup>

<sup>1</sup> *State Key Laboratory of Transient Optics and Photonics, Xi'an Institute of Optics and Precision Mechanics, Chinese Academy of Sciences, Xi'an 710119, China*

<sup>2</sup> *University of Chinese Academy of Sciences, Beijing 100049, China*

<sup>3</sup> *School of Electronics and Information, Northwestern Polytechnical University, Xi'an 710072, China*

<sup>4</sup> *Division of Electrical and Electronic Engineering, School of Engineering, London South Bank University, 103 Borough Road, London SE1 0AA, UK*

<sup>5</sup> *zhangja@lsbu.ac.uk*

\* *liuyuanshan@opt.ac.cn,*

**Abstract:** A passively mode-locked fiber laser with 1.03 GHz fundamental repetition rate and low noise performance is demonstrated. The compact and robust laser operates at a central wavelength of 1553.9 nm with a 3 dB spectral bandwidth of 7.9 nm and a temporal width of 550 fs. All the fibers and components used in the laser are polarization-maintaining (PM), so the output pulses are linearly polarized. The degree of polarization (DOP) of the optical pulses is measured to be 0.9994. The phase noise of the seventh harmonic (7.21 GHz) is measured and a low timing jitter of 11.7 fs is obtained by integrating the phase noise from 30 MHz down to 100 Hz. The noise performance is detailed analyzed and the methods for further optimizing the timing jitter are also proposed. So far as we know this is the first reported low noise all-PM erbium-doped fiber (EDF) laser with gigahertz level pulse repetition rate.

## Introduction

High repetition rate femtosecond lasers play an important role in many applications, including optical arbitrary waveform generation [1,2], high precision frequency metrology [3,4], ultrastable microwave signal generation [5-7], high speed optical sampling [8-10], and high resolution astronomical spectrographs (astrocombs) [11-14]. Over the past decade ultrafast lasers of multi-gigahertz repetition rate have been experimentally developed [15-27]. Recently an Yb-doped fiber laser with a fundamental repetition rate of 5 GHz is demonstrated, which is the highest fundamental pulse repetition rate at 1  $\mu\text{m}$  wavelength region [16]. Cheng et al. presents a gigahertz passively mode-locked 2  $\mu\text{m}$  fiber laser by using a homemade highly Tm-doped barium gallo-germanate glass fiber [19]. At a wavelength of around 1.55  $\mu\text{m}$ , a fiber laser with the highest fundamental repetition rate of 19.45 GHz is realized by Martinez. The laser is built by using heavily Er:Yb doped fiber as gain medium and mode-locked operation is achieved based on a carbon nanotube mode locker [21]. A stable, efficient, low timing jitter fiber laser with a repetition rate of 1 GHz is demonstrated by Byun et al. [24], which is monolithic and thermal-damage-free by inserting an undoped fiber piece between the

EDF and the butt-coupled saturable Bragg reflector (SBR). However, all the previously reported high-repetition-rate femtosecond lasers are designed and built based on non-PM fibers and components. In Thapa's work [26], although a piece of PM highly Er:Yb doped fiber is used in the 12 GHz fundamental repetition rate laser, other components are not PM types. Therefore, the polarization state of the output pulses is still undetermined. Recently, an 880 MHz Yb-doped mode-locked fiber laser with the lowest timing jitter (10 fs, integrated from 30 kHz to 5 MHz) is experimentally demonstrated. This is the first quantitative characterization of timing jitter in mode-locked fiber lasers with gigahertz-level repetition rate by using a high-precision balanced optical cross-correlation (BOC) technique [28]. The polarization state is of key importance in many polarization-dependent applications, for example, frequency doubling, four-wave mixing, cross-phase modulation, and so on. Besides, lasers based on PM fibers and components are insensitive to fiber twisting or bending as well as the environmental instability such as significant thermal and mechanical changes [12, 29]. Thus, EDF lasers based on PM fibers and components would be more suitable for harsh environment and more applications. Previously, passively mode-locked, PM fibers with low pulse repetition rate have been demonstrated [30-32]. However, PM EDF lasers with gigahertz level pulse repetition rate has not been reported so far as we know.

In this paper, we experimentally demonstrate an EDF laser with a fundamental pulse repetition rate of 1.03 GHz based on PM EDFs and components. The compact and robust laser operates at a central wavelength of 1553.9 nm with a 3 dB spectral bandwidth of 7.9 nm, and delivers optical pulses with 550 fs temporal width. The output light turns out to be linearly polarized and the measured DOP is up to 0.9994. The phase noise of the seventh harmonic (7.21 GHz) is measured and the timing jitter integrated from 100 Hz to 30 MHz is 11.7 fs. The noise performance is detailed analyzed and the optimization methods are proposed. By making the total net-cavity dispersion approach zero as nearly as possible, we eliminate the influence of the Gordon-Haus jitter and obtain the low jitter. To the best of our knowledge, the laser is the first all-PM femtosecond EDF laser with a low timing jitter and gigahertz level pulse repetition rate.

## Experimental Setup

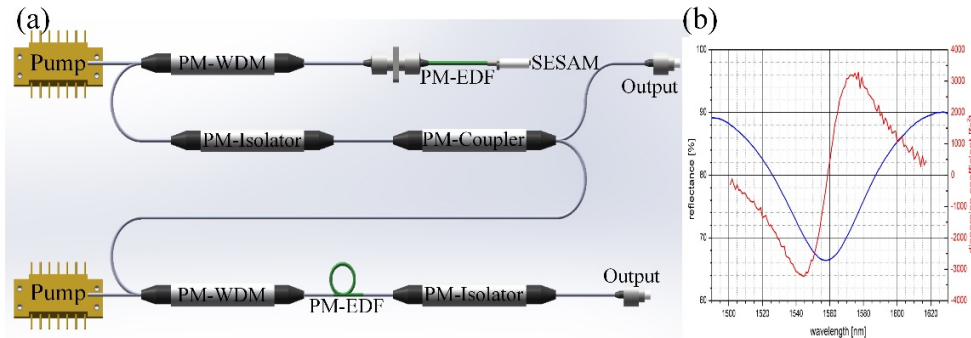


Fig.1. (a) Schematic experimental setup of the 1 GHz all-PM fiber laser. (b) The reflectance and dispersion of the SESAM.

A schematic diagram of the experimental setup is depicted in Fig. 1(a). The laser cavity consists of a 10 cm PM EDF, a coated fiber ferrule and a piece of semiconductor saturable absorbing mirror (SESAM). The fiber used in the experiment is Liekki Er80-4/125-PM which has a normal dispersion of 20.4 fs<sup>2</sup>/mm at 1554 nm. Both ends of the PM active fiber are glued in ceramic ferrules of 127  $\mu$ m inner diameter and flat polished. One end of the gain fiber is connected to a coated PM fiber ferrule through a mating sleeve. The coated PM fiber ferrule, as an output coupler, has a high reflectivity of 95% at 1550 nm as well as a high transmittance of over 98% at 976 nm to increase the pump efficiency. The other end of the fiber is

butt-coupled to a SESAM which is used as a mode-locker. The SESAM produced by Batop GmbH has 18% modulation depth, 30% absorbance, 5 ps recovery time and  $1 \text{ mJ/cm}^2$  damage threshold. As can be seen in Fig. 1(b), the anomalous dispersion of the SESAM (produced by Batop GmbH) is  $-1750 \text{ fs}^2$  at  $1553.9 \text{ nm}$ , which makes the net dispersion of the cavity is estimated to be  $\sim 0.002 \text{ ps}^2$ .

The pump light provided by a  $976 \text{ nm}$  laser diode is injected into the EDF through a PM wavelength division multiplexer (WDM) and the coated PM fiber ferrule. The optical pulses are outputted through a PM isolator which can eliminate the influence of unabsorbed pump light. The optical spectrum of the output light is measured by an optical spectrum analyzer (AQ6370D, YOKOGAWA). The radio spectrum is detected by a high-speed photodetector (UPD-15-IR2, ALPHALAS) and monitored by a signal analyzer (FSUP26, Rohde & Schwarz).

## Results and discussion

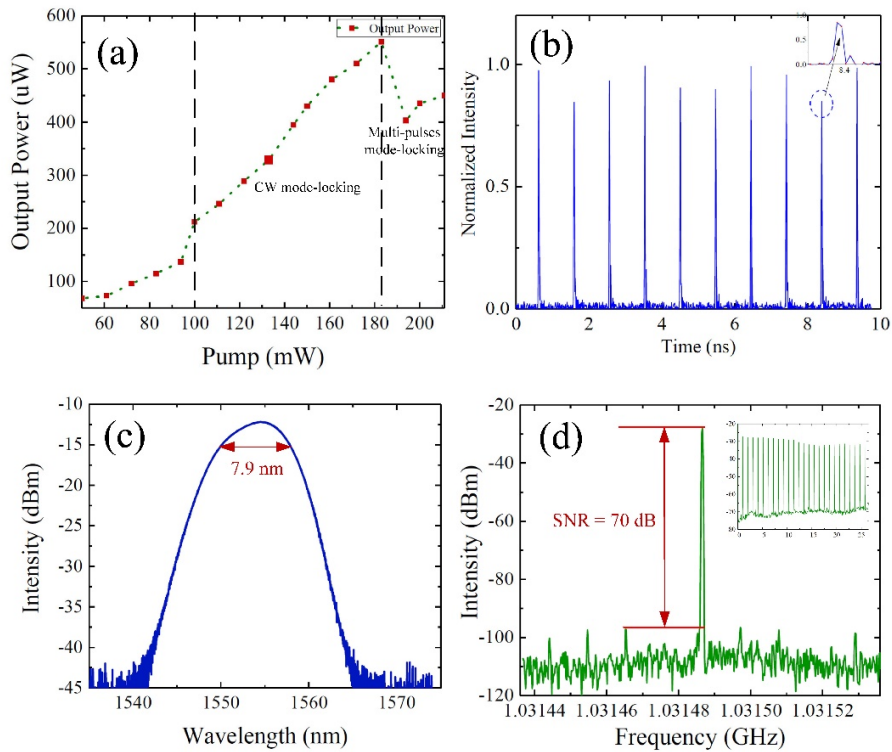


Fig. 2. (a) Output power versus the pump power. The mode-locking threshold pump power is  $100 \text{ mW}$ . (b) Oscilloscope trace of pulse train. (c) Optical spectrum. (d) RF spectrum with a  $200 \text{ Hz}$  RBW and  $300 \text{ Hz}$  VBW. Inset: RF spectrum with a broad span.

The dependence of the output power on the input pump power is illustrated in Fig. 2(a) for different operation regimes. Stable continuous wave (CW) mode-locked state with an output power of  $220 \mu\text{W}$  is realized at a threshold pump power of  $100 \text{ mW}$ . When the pump power increases to  $183 \text{ mW}$ , the output power grows linearly to  $550 \mu\text{W}$ . However, as the pump power is further increased over  $183 \text{ mW}$ , the  $3 \text{ dB}$  spectral bandwidth suddenly gets narrower (e.g., from  $9.5 \text{ nm}$  to  $8.0 \text{ nm}$ ) and the output power reduces to  $400 \mu\text{W}$ , indicating a transition from CW to multi-pulses mode-locked states. H. Byun et al have investigated the thermal damage issue of the mode-locker [24] and their studies show that a higher pump power will lead to more residual pump light at the surface of the mode-locker which could cause thermal

damage to the mode-locker when it is directly contacted to the EDF. In this work, due to the low pump power and high absorption of the gain fiber, the SESAM is protected from thermal damage which is helpful for the stable mode-locked operation of the laser. The oscilloscope trace of the output pulses is given in Fig. 2(b), the corresponding temporal period is 969.47 ps, indicating the fundamental cavity frequency of 1.03 GHz. The fluctuation of the peak values is caused by the insufficient sampling rate, the details of the sampled pulses can be seen in the inset where the red square dot is the sampling point. Figure 2(c) shows the optical spectrum of the optical pulses at 510  $\mu$ W output power. The central wavelength is 1553.9 nm with a 3 dB spectral bandwidth of 7.9 nm. The radio frequency (RF) spectrum shown in Fig. 2(d) indicates a fundamental pulse repetition rate of 1.03 GHz with 70 dB signal-to-noise ratio (SNR). The results are directly detected by using the signal analyzer (FSUP26, Rohde & Schwarz) at a 200 Hz resolution bandwidth (RBW), a 300 Hz video bandwidth (VBW) and a 100 kHz span. The inset of Fig. 2(d) depicts the RF spectrum of all harmonics in a broad span of 26.5 GHz. The mode-locked waveform of the oscilloscope trace and the clear intensity of the RF spectrum demonstrate that the oscillator is operating at CW mode-locked state.

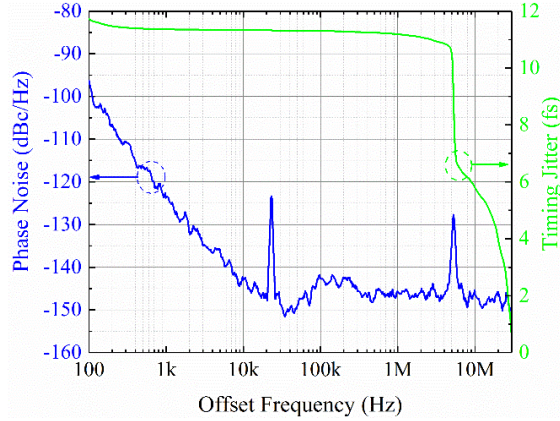


Fig. 3. The SSB phase noise of the 7th harmonic frequency and the integrated timing jitter.

The single sideband (SSB) phase noise is directly measured by using the method proposed in [33]. According to the analyses present in [33, 34], the phase noises measured at the fundamental frequency and lower harmonics are strongly influenced by the intensity noise of the laser. However, for higher harmonics the phase noise rises proportionally to  $k^2$ , where  $k$  is the order of harmonic frequency. Besides, the shot-noise level of the measuring system also increases when measuring high carrier frequency. Therefore, to characterize the timing jitter performance of the laser as accurately as possible, we choose to measure the SSB phase noise at the 7th harmonic frequency (7.21 GHz). The phase noise and corresponding timing jitter are displayed in Fig. 3 and the timing jitter is calculated to be 11.7 fs by integrating from 30 MHz down to 100 Hz, which confirms that the presented high repetition rate EDF laser has a low noise performance. As can be seen that the phase noise at 100 Hz offset frequency is -97 dBc/Hz and decreases to -143 dBc/Hz with a near -20 dB/decade slope while the offset frequency increases to 10 kHz. For the offset frequency higher than 10 kHz, the phase noise fluctuates between -140 and -150 dBc/Hz. The phase noise at high offset frequency is limited by the short-noise floor of the measuring system. If the BOC technique [35, 36] is used in the measurement, we can anticipate a better timing jitter of fs-level. Based on the theory models and experimental results in [37-39], the -20 dB/decade decreasing slope at low offset frequency shows that the timing jitter of this laser is dominated by the amplified spontaneous emission (ASE) noise, which originates from the high gain fiber and intra-cavity losses. The ASE noise contributes to the timing jitter via two different ways: (i) the direct effect that the ASE noise causes a random shift of the pulse temporal position, (ii) the indirect effect that the ASE noise causes the fluctuation of the center frequency of the optical pulses which can be

further transferred to timing jitter via the intra-cavity dispersion, namely Gordon-Haus jitter. Two aspects contribute to the intra-cavity dispersion: (i) the gain fiber, (ii) the SESAM. The dispersion of the gain fiber at the wavelength around 1555 nm is nearly unchanged. However, from Fig.1(b), we can see that the dispersion of the SESAM in the range from 1545 to 1570 nm is dramatically wavelength-dependent with a positive slope of  $250 \text{ fs}^2/\text{nm}$ . The central wavelength of the laser is carefully tuned toward short wavelength by adjusting the pump power, so that the SESAM can provide large anomalous dispersion to compensate the normal dispersion from the EDF. Thus the total net-cavity dispersion can approach to zero as nearly as possible. As a result, the Gordon-Haus jitter is eliminated, which is an important reason for this laser achieving such a low timing jitter. The timing jitter can be further improved by optimizing the parameters and structure of the laser. Due to the compact structure of the laser, there is only PM fiber inside the cavity and the PM components are all laid outside the cavity. We think this arrangement can lead to the increase of timing jitter. While the optical signal is polarized along the slow-axis of the PM fiber, the ASE noise in the fast-axis polarization is also amplified and might influence the stable CW mode-locking, which directly increases the timing jitter. Actually, a polarizer could be used inside the cavity so that the direct influence of the ASE noise can be reduced and the timing jitter will be decreased. Besides, the timing jitter can be reduced by increasing the pulse energy, shortening the pulse duration, and decreasing the cavity losses [37]. Also, a SESAM with lower non-saturable loss and smaller recovery time can also improve the timing jitter performance.

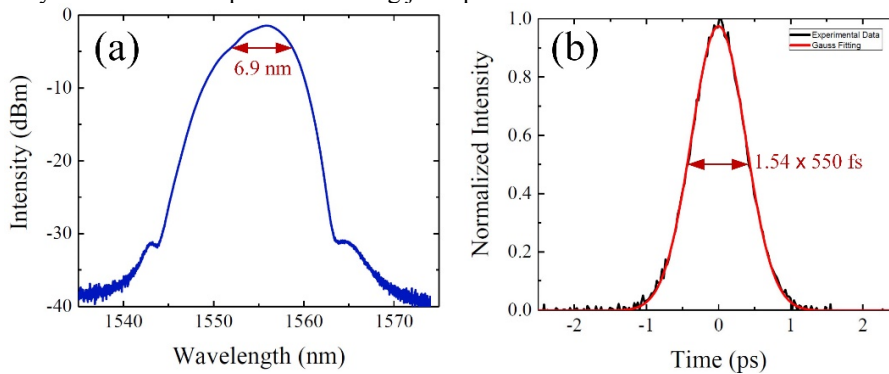


Fig. 4. (a) Optical spectrum measured after the low-noise amplifier. (b) The measured intensity autocorrelation trace.

The optical power is amplified to 5.5 mW in order to measure the pulse intensity autocorrelation trace (measured by HAC-200, Alnair Labs). As shown in Fig. 4(a), the amplified pulses has a 3 dB spectral bandwidth of 6.9 nm implying a transform-limited pulse duration of 515 fs. The measured intensity autocorrelation trace is shown in Fig. 4(b) which gives a full width at half maximum (FWHM) width of 850 fs. If a Gaussian-shape pulse is assumed, the pulse duration is calculated to be 550 fs, the measured pulse duration is well consistent with the transform-limited pulse duration.

All the components consisted in the experimental setup are PM types with fast axes blocked, thus we obtain the linearly polarized output pulses. The polarization state of these pulses is measured by using a polarization measurement system (PSG-101A, General Photonics Corp). As shown in Fig. 5 the measured normalized Stokes parameters are  $S_1:-0.9972$ ,  $S_2:-0.0752$ ,  $S_3:-0.0055$ , respectively. The corresponding DOP is calculated to be 0.9994, which make this laser suitable for many polarization-dependent applications.

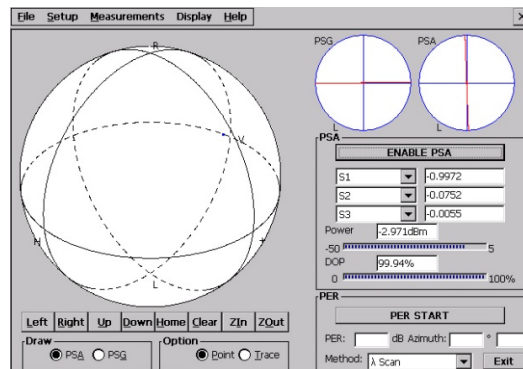


Fig. 5. The measured polarization state of the output pulse.

## Conclusion

In conclusion, we present a passively mode-locked EDF laser with a fundamental repetition rate of 1.03 GHz. The laser operates at a central wavelength of 1553.9 nm and delivers 550 fs mode-locked pulses. To decouple the intensity noise, the phase noise of the seventh harmonic is measured and the timing jitter is calculated to be 11.7 fs by integrating the phase noise from 30 MHz down to 100 Hz. We analyzed the noise performance and eliminate the influence of the Gordon-Haus jitter by making the total net-cavity dispersion approach zero as nearly as possible. Thus a low timing jitter is obtained and the methods for further optimization are also proposed. All the fibers and components used in the laser are PM types resulting in a linearly polarized output light with a DOP of 0.9994. So far as we know, this is the first reported low noise all-PM femtosecond EDF laser with over 1 GHz pulse repetition rate and linearly polarized output pulses. The presented laser with compact and robust structure guarantees the great potential in many applications, such as low noise astrocomb systems.

## Funding

This work was supported by National key R&D Program of China (2016YFF0200700) and Natural Science Foundation of China (61875226).

## References

- [1] S. T. Cundiff, and A. M. Weiner 2010 *Nat. Photonics* **4** 760-6
- [2] A. Rashidinejad, D. E. Leaird, and A. M. Weiner 2017 *Opt. Express* **23** 12265-73
- [3] D. J. Jones, S. A. Diddams, J. K. Ranka, A. Stentz, R. S. Windeler, J. L. Hall, and S. T. Cundiff 2000 *Science* **288** 635-40
- [4] T. M. Fortier, A. Bartels, and S. A. Diddams 2013 *Opt. Lett.* **31** 1011-3
- [5] T. M. Fortier, M. S. Kirchner, F. Quinlan, J. Taylor, J. C. Bergquist, T. Rosenband, N. Lemke, A. Ludlow, Y. Jiang, C. W. Oates, and S. A. Diddams 2011 *Nat. Photonics* **5** 425-9
- [6] T. M. Fortier, A. Rolland, F. Quinlan, F. N. Baynes, A. J. Metcalf, A. Hati, A. D. Ludlow, N. Hinkley, M. Shimizu, T. Ishibashi, J. C. Campbell, and S. A. Diddams 2016 *Laser Photonics Rev.* **10** 780-90
- [7] H. Jiang, J. Taylor, F. Quinlan, T. Fortier, and S. A. Diddams 2011 *IEEE Photon. J.* **3** 1004-12
- [8] J. Kim, M. J. Park, M. H. Perrott, F. X. Kärtner 2008 *Opt. Express* **16** 16509-15
- [9] V. Vercesi, D. Onori, J. Davies, A. Seeds, and C. P. Liu 2017 *Opt. Express* **25** 29249-59
- [10] H. Meng, J. Leng, C. Qian, and J. Zhao 2017 *J. Opt. Soc. Am. B* **34** 824-30
- [11] R. A. McCracken, J. M. Charsley, and D. T. Reid 2017 *Opt. Express* **25** 15058-78
- [12] M. Lezius, T. Wilken, C. Deutsch, M. Giunta, O. Mandel, A. Thaller, V. Schkolnik, M. Schiemanck, A. Dinkelaker, A. Kohfeldt, A. Wicht, M. Krutzik, A. Peters, O. Hellmig, H. Duncker,

- K. Sengstock, P. Windpassinger, K. Lampmann, T. Hülasing, T. W. Hänsch, and R. Holzwarth 2016 *Optica* **3** 1381–7
- [13] V. Torres-Company, and A. M. Weiner 2014 *Laser Photonics Rev.* **8** 368–93
- [14] P. Zou, T. Steinmetz, A. Falkenburgher, Y. Wu, L. Fu, M. Mei, R. Holzwarth 2016 *Journal of Applied Mathematics and Physics* **04** 202-5
- [15] H.-W. Chen, G. Chang, S. Xu, Z. Yang, and F. X. Kärtner 2012 *Opt. Lett.* **37** 3522–4
- [16] H. Cheng, W. Wang, Y. Zhou, T. Qiao, W. Lin, S. Xu, and Z. Yang 2017 *Opt. Express* **25** 27646-51
- [17] C. Li, G. Wang, T. Jiang, A. Wang, Z. Zhang, A. M. Wang, and Z. G. Zhang 2013 *Opt. Lett.* **38** 314–6
- [18] B. Xu, H. Yasui, Y. Nakajima, Y. Ma, Z. G. Zhang, and K. Minoshima 2017 *Opt. Express* **25** 11910-8
- [19] H. Cheng, W. Lin, Z. Luo, and Z. Yang 2018 *IEEE J. Sel. Top. Quantum Electron.* **24** 1100106
- [20] H. Cheng, W. Lin, T. Qiao, S. Xu, and Z. Yang 2016 *Opt. Express* **24** 29882–95
- [21] A. Martinez and S. Yamashita 2011 *Opt. Express* **19** 6155-63
- [22] A. Martinez and S. Yamashita 2012 *Appl. Phys. Lett.* **101** 041118
- [23] S. Y. Set, S. Yamashita, K. Hsu, K. H. Fong, Y. Inoue, K. Sato, D. Tanaka, and M. Jablonski 2018 *IEEE Photonics Technol. Lett.* **17** 750–2
- [24] H. Byun, M. Y. Sander, A. Motamedi, H. Shen, G. S. Petrich, L. A. Kolodziejski, E. P. Ippen, and F. X. Kärtner 2010 *Appl. Opt.* **49** 5577–82
- [25] H. Byun, D. Pudo, J. Chen, E. P. Ippen, and F. X. Kärtner 2008 *Opt. Lett.* **33** 2221-3
- [26] R. Thapa, D. Nguyen, J. Zong, and A. Chavez-Pirson 2014 *Opt. Lett.* **39** 1418–21
- [27] J. J. McFerran, L. Nenadović, W. C. Swann, J. B. Schlager, and N. R. Newbury 2007 *Opt. Express* **15** 13155-66
- [28] Y. Wang, H. Tian, Y. Ma, Y. Song, and Z. Zhang 2018 *Opt. Lett.* **43** 4382-5
- [29] J. Lee, K. Lee, Y. Jang, H. Jang, S. Han, S. Lee, K. Kang, C. Lim, Y. Kim, and S. Kim 2014 *Sci. Rep.* **4** 5134
- [30] G. Sobon, J. Sotor, and K.M. Abramski 2012 *Laser Phys. Lett.* **9** 581-5
- [31] H. Jang, Y. Jang, S. Kim, K. Lee, S. Han, Y. Kim, and S. Kim 2015 *Laser Phys. Lett.* **12** 105102-7
- [32] G. Sobon, J. Sotor, I. Pasternak, K. Krzempek, W. Strupinski, and K. M. Abramski 2013 *Laser Phys.* **23** 125101-4
- [33] D. von der Linde 1986 *Appl. Phys. B* **39** 201-17
- [34] H. A. Haus, and A. Mecozzi 1993 *IEEE J. Quantum Electron.* **29** 983–4
- [35] T. R. Schibli, J. Kim, O. Kuzucu, J. T. Gopinath, S. N. Tandon, G. S. Petrich, L. A. Kolodziejski, J. G. Fujimoto, E. P. Ippen, and F. X. Kärtner 2003 *Opt. Express* **28** 947-3
- [36] J. Kim, J. Chen, Z. Zhang, F. N. C. Wong, F. X. Kärtner, F. Loehl and H. Schlarb 2007 *Opt. Lett.* **32** 1044-3
- [37] R. Paschotta 2004 *Appl. Phys. B* **79** 153–10
- [38] R. Paschotta 2004 *Appl. Phys. B* **79** 163–11
- [39] R. Paschotta 2010 *Opt. Express* **18** 5041-14